2024 IEEE 63rd Conference on Decision and Control (CDC)
December 16-19, 2024. MiCo, Milan, Italy

Robust rigid-body attitude backstepping control

Arthur H. D. Nunes, Guilherme V. Raffo, Leonardo A. B. Torres, Luciano C. A. Pimenta

Abstract— **In this work, we present a rigid-body attitude control strategy for tracking desired time-varying orientation under unknown-but-bounded disturbances. The control scheme aims to achieve nominal performance and disturbance attenuation. Initially, a nominal controller is designed to guarantee asymptotically convergence of the error between nominal and reference orientations to the origin in the absence of disturbances, ensuring nominal system performance. Thereafter, considering unknown-but-bounded disturbances, an auxiliary robust adaptive backstepping control approach based on projection modification is employed to ensure the maximum tracking error deviation is ultimately bounded and the adaptive parameters remain bounded. Experimental results with a nano quadcopter corroborate our proposed control strategy.**

I. INTRODUCTION

The control of rigid-body attitude plays a crucial role in various engineering applications, ranging from spacecraft maneuvering to aerial robotics and autonomous vehicles [1], [2], [3], [4], [5]. These systems are characterized by their ability to change their orientation in a three-dimensional space. They are usually prone to the presence of disturbances, which can arise from environmental factors, external forces, and inherent uncertainties in the modeled system dynamics. Achieving accurate robust attitude tracking is essential for ensuring stability, performance, and safety of such systems in their main applications. Especially Unmanned Aerial Vehicles (UAVs), usually require the attitude tracking to allow aggressive maneuvers while ensuring flight stability in disturbed scenarios.

In recent years, extensive research has been conducted to address the challenges associated with attitude control of rigid bodies. Traditional methods for regulation problems, such as PID and LQR controllers, have been widely employed to achieve performance of the nominal system under ideal conditions [6], [7]. However, these approaches are often based on linearized models, which lead to poor performance, in addition to not allowing the execution of aggressive maneuvers. Additionally, controllers designed only for ideal conditions often struggle to maintain satisfactory performance when subjected to disturbances.

The authors are with the Graduation Program in Electrial Engineering (PPGEE) of the Universidade Federal de Minas Gerais (UFMG), Belo Horizonte, MG, 31270-901, Brazil (emails: arthurhdn@ufmg.br; raffo@ufmg.br; leotorres@ufmg.br; lucpim@cpdee.ufmg.br).

This work was in part supported by the project INCT (National Institute of Science and Technology) under the grant CNPq (Brazilian National Research Council) 465755/2014-3, FAPESP (São Paulo Research Foundation) 2014/50851-0 and FAPEMIG (under grants APQ-02144-18 and APQ-00630-23). This work was also supported in part by the Brazilian agencies Coordination for the Improvement of Higher Education Personnel (CAPES) through the Academic Excellence Program (PROEX), and CNPq (grant numbers 309925/2023-1, 317058/2023-1 and 422143/2023-5).

To overcome these limitations, advanced control schemes have been proposed, aiming to integrate nominal performance with disturbance attenuation capabilities through the utilization of both nonlinear and robust control techniques. The compromise idea is to design controllers that ensure asymptotic stability under nominal conditions while also possessing the ability to mitigate the effects of disturbances [8], [9], [10]. Although those works use this idea, none of them employ backstepping.

In a previous recent work [11], we have proposed a backstepping controller with integral action to control a quadcopter with rigid-body attitude dynamics. This controller has allowed constant disturbance rejection. The backstepping technique has been widely used as a nominal controller, especially for aerial robots [12], [13], [14], [15], [16], [17].

Now, we extend our previous controller by proposing a robust adaptive backstepping control scheme to mitigate not only constant disturbances but any norm-bounded ones, aiming to better address the challenges of tracking orientation references. The proposed control scheme leverages the combination of a nominal controller and a robust adaptive control approach for disturbances, enabling the system to achieve robustness in the face of uncertainties while tracking a time-varying reference attitude.

Accordingly, the nominal controller is designed to ensure the asymptotic convergence of the error between the nominal and reference orientations to the origin in the absence of disturbances. Recognizing the practical reality that disturbances are almost inevitable, we introduce a robust adaptive backstepping control approach to mitigate their effects. The controller allows the system to approach the nominal trajectory while bounding the maximum deviation [10].

In this sense, the proposed method is similar to the work [18], which has inspired the current development. In [18], the authors have proposed a guaranteed cost control with a robust adaptive auxiliary controller to solve the origin regulation problem. However, their solution cannot solve the tracking problem and allows adaptive gains to drift towards infinity. To overcome these limitations, we employ a nonlinear nominal control law and a projection modification [19] on the adaptive gains. Our approach also differs in the orientation error calculation, employing a unit quaternion error representation instead of combinations of real and imaginary parts. In this way, it is possible to guarantee the tracking using the unit error quaternion, which holds properties of attitude quaternions.

979-8-3503-1632-2/24/$31.00 ©2024 IEEE

Overall, the main contribution of this work is a rigid-body attitude tracking controller with the following features: (i) guaranteed nominal stability; (ii) ultimate boundedness of the tracking error in the disturbed case; (iii) bounded evolution of the adaptive parameters; and (iv) validation through simulation and experimental results.

Notation

We adopt quaternion algebra in this work, where unit quaternions denote attitude. The main advantages of this algebra are the singularity-free attitude representation, the easier coupling between complex systems, and some similarities with vector representations [20], [21], [22], [23].

For any quaternion $\boldsymbol{o} \in \mathbb{H}$, with $\boldsymbol{o} = o_0 + o_{\mathrm{x}}\hat{\imath} + o_{\mathrm{y}}\hat{\jmath} + o_{\mathrm{z}}\hat{k}$, its real part is $\mathcal{R}\{\boldsymbol{o}\} = o_0 \in \mathbb{R}$, and its imaginary part is the pure quaternion (with null real part) $\mathcal{I}\{\boldsymbol{o}\} = o_{\mathrm{x}}\hat{\imath} + o_{\mathrm{y}}\hat{\jmath} + o_{\mathrm{z}}\hat{k} \in \mathbb{H}_p$, such that $\hat{\imath}\hat{\jmath} = \hat{k}$, $\hat{\jmath}\hat{k} = \hat{\imath}$, $\hat{k}\hat{\imath} = \hat{\jmath}$, $\hat{\imath}\hat{\jmath}\hat{k} = -1$. The conjugation operation is denoted by $\boldsymbol{o}^* = \mathcal{R}\{\boldsymbol{o}\} - \mathcal{I}\{\boldsymbol{o}\}$. In this paper, given pure quaternions $\boldsymbol{a}, \boldsymbol{b} \in \mathbb{H}_{\mathrm{p}}$, we define the operations $\boldsymbol{a} \times \boldsymbol{b}$ and $\boldsymbol{a}^\top \boldsymbol{b}$ as the usual cross and inner products for the vectors associated with their imaginary parts; and the operation $\boldsymbol{b} = M\boldsymbol{a}$, with $M \in \mathbb{R}^{3\times 3}$, as the usual matrix multiplication $[b_{\mathrm{x}}, b_{\mathrm{y}}, b_{\mathrm{z}}]^\top = M[a_{\mathrm{x}}, a_{\mathrm{y}}, a_{\mathrm{z}}]^\top$.

II. PROBLEM STATEMENT

Let $\boldsymbol{o} = \cos(\frac{\phi}{2}) + \boldsymbol{n}\sin(\frac{\phi}{2}) \in \mathbb{H}$ be the attitude unit quaternion in terms of the rotation angle $\phi \in \mathbb{S}$, where $\mathbb{S}$ is the circle space, around the axis given by the pure quaternion $\boldsymbol{n} = n_{\mathrm{x}}\hat{\imath} + n_{\mathrm{y}}\hat{\jmath} + n_{\mathrm{z}}\hat{k} \in \mathbb{H}_p$, with $\|\boldsymbol{n}\| = 1$. Let $\boldsymbol{\omega} = \omega_{\mathrm{x}}\hat{\imath} + \omega_{\mathrm{x}}\hat{\jmath} + \omega_{\mathrm{x}}\hat{k} \in \mathbb{H}_p$ be the angular velocity of the body-fixed reference frame w.r.t. the inertial reference frame, expressed in the body-fixed reference frame. A rigid-body attitude evolves with time according to

$$\dot{\boldsymbol{o}} = \frac{1}{2}\boldsymbol{o}\boldsymbol{\omega}, \tag{1}$$

$$\dot{\boldsymbol{\omega}} = \boldsymbol{\Omega} + J^{-1}\boldsymbol{\tau} + J^{-1}\boldsymbol{\tau}_d, \quad \boldsymbol{\Omega} = -J^{-1}(\boldsymbol{\omega} \times J\boldsymbol{\omega}), \tag{2}$$

where $\boldsymbol{\tau} \in \mathbb{H}_p$ is the control input, $\boldsymbol{\tau}_d \in \mathbb{H}_p$ is the disturbance, and $J = J^\top > 0 \in \mathbb{R}^{3\times 3}$ is the inertia tensor. This system is called the **practical system**.

The problem addressed in this work is the attitude trajectory tracking, formalized below.

Problem 1 (Attitude trajectory tracking): Given the rigid-body attitude system (1)-(2) with unknown-but-bounded disturbance $\boldsymbol{\tau}_d$, design a controller that drives the system asymptotically to a small neighborhood around a given reference trajectory $\boldsymbol{o}_{\mathrm{d}}(t)$ given by

$$\dot{\boldsymbol{o}}_{\mathrm{d}} = \frac{1}{2}\boldsymbol{o}_{\mathrm{d}}\boldsymbol{\omega}_{\mathrm{d}}, \tag{3}$$

such that $\boldsymbol{o}_d(0) = \boldsymbol{o}_{d,0}$ and $\boldsymbol{\omega}_d(t)$ are known, with $\boldsymbol{\omega}_{\mathrm{d}} \in \mathbb{H}_{\mathrm{p}}$ defined as the desired angular velocity of the target reference frame w.r.t. the inertial reference frame, expressed in the target reference frame. In other words, find a control law $\boldsymbol{\tau}$ such that $\boldsymbol{o}(t)$ converges to a positively invariant set around $\boldsymbol{o}_{\mathrm{d}}(t)$, even in the presence of disturbances.

III. PROPOSED CONTROLLER

Our approach to address Problem 1 is inspired by [18], while also incorporating several crucial additional elements that have not been previously considered. Besides using a multiplicative quaternion error as the basis for our theoretical development, we provide experimental results and consider time-varying reference attitude with guaranteed upper bounds for the adaptive parameters. This last feature turns out to be a requirement for any practical implementation.

Our control design methodology consists of three steps. First, we find a nominal (*i.e.* when $\boldsymbol{\tau}_{\mathrm{d}} = 0$) feedback controller that ensures nominal asymptotic convergence to the reference $\boldsymbol{o}_{\mathrm{d}}(t)$. One advantage of our controller w.r.t. the strategy in [18] is that we solve the nominal control problem for a given time-varying reference trajectory $\boldsymbol{o}_{\mathrm{d}}(t)$ rather than only solving the regulation problem ($\boldsymbol{o}_{\mathrm{d}} \equiv 1$). Thereafter, we formulate a robust adaptive control law to mitigate the error between the practical system and the previously determined nominal trajectory, ensuring that the tracking error converges to a small neighborhood around the origin. By implementing a projection modification in the adaptation law of the gains, we prevent these gains from drifting towards infinity, as would invariably occur in practical scenarios. Finally, we obtain the practical system control law by combining the nominal and robust adaptive controllers.

A. Nominal controller

We define the **nominal system**, as (1)-(2) when $\boldsymbol{\tau}_d = 0$. The corresponding variables are represented with a top bar, such that

$$\dot{\bar{\boldsymbol{o}}} = \frac{1}{2}\bar{\boldsymbol{o}}\bar{\boldsymbol{\omega}}, \tag{4}$$

$$\dot{\bar{\boldsymbol{\omega}}} = \quad \bar{\boldsymbol{\Omega}} + J^{-1}\bar{\boldsymbol{\tau}}, \quad \bar{\boldsymbol{\Omega}} = -J^{-1}(\bar{\boldsymbol{\omega}} \times J\bar{\boldsymbol{\omega}}). \tag{5}$$

The first part of our method is achieved based on the following Lemma.

Lemma 1: Let $\boldsymbol{e} \equiv \boldsymbol{o}_{\mathrm{d}}^*\bar{\boldsymbol{o}}$ be the attitude error quaternion between reference and nominal attitudes, with $\boldsymbol{z}_o \equiv \mathcal{I}\{\boldsymbol{e}\} \in \mathbb{H}_{\mathrm{p}}$ and the reference attitude $\boldsymbol{o}_d(t)$ evolving according to (3). Define $\boldsymbol{z}_\omega = \bar{\boldsymbol{\omega}} - \boldsymbol{\omega}_{\mathrm{d},\bar{\mathrm{B}}}$, where the representation of the reference angular velocity $\boldsymbol{\omega}_{\mathrm{d}}$ in the body-fixed reference frame of the nominal system is given by $\boldsymbol{\omega}_{\mathrm{d},\bar{\mathrm{B}}} = \boldsymbol{e}^*\omega_{\mathrm{d}}\boldsymbol{e}$. The nominal system asymptotically tracks the reference attitude if the control law is defined as

$$\bar{\boldsymbol{\tau}} = \bar{\boldsymbol{\omega}} \times J\bar{\boldsymbol{\omega}} + J\dot{\boldsymbol{\omega}}_{\mathrm{d},\bar{\mathrm{B}}} + J\bar{\boldsymbol{\tau}}_L, \tag{6}$$

$$\bar{\boldsymbol{\tau}}_L = -k_{\mathrm{o}}\boldsymbol{z}_o - K_\omega \boldsymbol{z}_\omega, \tag{7}$$

with $k_{\mathrm{o}} \in \mathbb{R}$, $k_{\mathrm{o}} > 0$, $K_\omega \in \mathbb{R}^{3\times 3}$, $K_\omega = K_\omega^\top > 0$.

Proof: Notice that the attitude error quaternion $\boldsymbol{e}$ represents the orientation of the target reference frame w.r.t. the body-fixed reference frame of the nominal system, in the sense that $\boldsymbol{a}_{\bar{\mathrm{B}}} = \boldsymbol{e}^*\boldsymbol{a}_{\mathrm{d}}\boldsymbol{e}$ for any pure quaternions $\boldsymbol{a}_{\bar{\mathrm{B}}}$ and $\boldsymbol{a}_{\mathrm{d}}$ representing the same vector w.r.t. the body-fixed nominal reference frame and the target reference frame, respectively. A complete alignment between these two reference frames means that $\bar{\boldsymbol{o}} = \boldsymbol{o}_\mathrm{d}$, and therefore, $\boldsymbol{e} = \boldsymbol{o}_\mathrm{d}^*\bar{\boldsymbol{o}} = 1$. The time derivative of the error is given by

$$\begin{aligned}\dot{\boldsymbol{e}} &= \dot{\boldsymbol{o}}_\mathrm{d}^*\bar{\boldsymbol{o}} + \boldsymbol{o}_\mathrm{d}^*\dot{\bar{\boldsymbol{o}}} = \left(\frac{1}{2}\boldsymbol{o}_\mathrm{d}\boldsymbol{\omega}_\mathrm{d}\right)^*\bar{\boldsymbol{o}} + \boldsymbol{o}_\mathrm{d}^*\left(\frac{1}{2}\bar{\boldsymbol{o}}\bar{\boldsymbol{\omega}}\right),\\ &= \frac{1}{2}\boldsymbol{\omega}_\mathrm{d}^*\boldsymbol{o}_\mathrm{d}^*\bar{\boldsymbol{o}} + \frac{1}{2}\boldsymbol{o}_\mathrm{d}^*\bar{\boldsymbol{o}}\bar{\boldsymbol{\omega}} = -\frac{1}{2}\boldsymbol{\omega}_\mathrm{d}\boldsymbol{e} + \frac{1}{2}\boldsymbol{e}\bar{\boldsymbol{\omega}}.\end{aligned}$$

By considering $\boldsymbol{\omega}_{\mathrm{d},\bar{\mathrm{B}}} = \boldsymbol{e}^*\boldsymbol{\omega}_\mathrm{d}\boldsymbol{e}$ in the previous expression, we have that

$$\dot{\boldsymbol{e}} = \frac{1}{2}\boldsymbol{e}\left(\bar{\boldsymbol{\omega}} - \boldsymbol{\omega}_{\mathrm{d},\bar{\mathrm{B}}}\right) = \frac{1}{2}\boldsymbol{e}\boldsymbol{z}_\omega, \tag{8}$$

with $\boldsymbol{z}_\omega = \bar{\boldsymbol{\omega}} - \boldsymbol{\omega}_{\mathrm{d},\mathrm{B}}$. Denoting $\mathcal{R}\{\boldsymbol{e}\} = z_o$, and using $\mathcal{I}\{\boldsymbol{e}\} = \boldsymbol{z}_o$, one has that $\boldsymbol{e} = z_o + \boldsymbol{z}_o$, and the last expression can be rewritten as

$$\dot{z}_o = -\frac{1}{2}\boldsymbol{z}_o^\top\boldsymbol{z}_\omega, \quad \dot{\boldsymbol{z}}_o = \frac{1}{2}\left(z_o\boldsymbol{z}_\omega + \boldsymbol{z}_o \times \boldsymbol{z}_\omega\right). \tag{9}$$

Conversely, from (5), we obtain

$$\dot{\boldsymbol{z}}_\omega = \bar{\boldsymbol{\Omega}} + J^{-1}\bar{\boldsymbol{\tau}} - \dot{\boldsymbol{\omega}}_{\mathrm{d},\mathrm{B}}.$$

By choosing $\bar{\boldsymbol{\tau}}$ from (6), we have that

$$\dot{\boldsymbol{z}}_\omega = -k_\mathrm{o}\boldsymbol{z}_o - K_\omega\boldsymbol{z}_\omega. \tag{10}$$

Using the following candidate Lyapunov function:

$$V(\boldsymbol{e}, \boldsymbol{z}_\omega) = k_\mathrm{o}\boldsymbol{z}_o^\top\boldsymbol{z}_o + k_\mathrm{o}(1 - z_o)^2 + \frac{1}{2}\boldsymbol{z}_\omega^\top\boldsymbol{z}_\omega, \tag{11}$$

yields

$$\begin{aligned}\dot{V} &= 2k_\mathrm{o}\boldsymbol{z}_o^\top\left[\frac{1}{2}\left(z_o\boldsymbol{z}_\omega + \boldsymbol{z}_o \times \boldsymbol{z}_\omega\right)\right]\\ &\quad - 2k_\mathrm{o}(1 - z_o)\left(-\frac{1}{2}\boldsymbol{z}_o^\top\boldsymbol{z}_\omega\right) + \boldsymbol{z}_\omega^\top\left[-k_\mathrm{o}\boldsymbol{z}_o - K_\omega\boldsymbol{z}_\omega\right],\\ \dot{V} &= -\boldsymbol{z}_\omega^\top K_\omega\boldsymbol{z}_\omega \leq 0.\end{aligned} \tag{12}$$

Notice that $\dot{V} = 0 \Leftrightarrow \boldsymbol{z}_\omega = 0$, and the equilibrium point $(\boldsymbol{z}_o = 0, \boldsymbol{z}_\omega = 0, z_o^2 = 1 - \|\boldsymbol{z}_o\|^2 = 1)$ is the only element in the largest positively invariant set where $\dot{V} = 0$, as it can be verified from the attitude error system dynamics given by (9) and (10). By LaSalle's invariance principle [24, Corollary 4.2], the attitude error will converge asymptotically to the equilibrium point, and $\boldsymbol{e} = z_o + \boldsymbol{z}_o \to 1 \Leftrightarrow \boldsymbol{o} \to \bar{\boldsymbol{o}}_\mathrm{d}$. ■

B. Robust adaptive backstepping control

For the second part of our methodology, we propose a robust adaptive backstepping control law to stabilize the error between the practical (1)-(2) and nominal (4)-(5) systems. Comparing both, the **error system** describes the mismatch between them.

Let $\boldsymbol{o}_e = \bar{\boldsymbol{o}}^*\boldsymbol{o}$ be the error between the practical and nominal orientations. Accordingly, we obtain

$$\dot{\boldsymbol{o}}_e = -\frac{1}{2}\bar{\boldsymbol{\omega}}\boldsymbol{o}_e + \frac{1}{2}\boldsymbol{o}_e\boldsymbol{\omega}.$$

By considering the nominal angular velocity w.r.t. the inertial reference expressed in the body-fixed frame $\bar{\boldsymbol{\omega}}_\mathrm{B} = \boldsymbol{o}_e^*\bar{\boldsymbol{\omega}}\boldsymbol{o}_e$, yields

$$\dot{\boldsymbol{o}}_e = \frac{1}{2}\boldsymbol{o}_e\boldsymbol{\omega}_e, \tag{13}$$

where $\boldsymbol{\omega}_e = \boldsymbol{\omega} - \bar{\boldsymbol{\omega}}_B$. Also, we have that

$$\begin{aligned}\dot{\boldsymbol{\omega}}_e &= \dot{\boldsymbol{\omega}} - \dot{\bar{\boldsymbol{\omega}}}_B,\\ \dot{\boldsymbol{\omega}}_e &= \boldsymbol{\Omega}_e + J^{-1}\boldsymbol{\tau}_d + J^{-1}\boldsymbol{\tau} - J^{-1}\bar{\boldsymbol{\tau}}_B,\end{aligned} \tag{14}$$

where $\boldsymbol{\Omega}_e = \boldsymbol{\Omega} - \boldsymbol{o}_e^*\bar{\boldsymbol{\Omega}}\boldsymbol{o}_e + \boldsymbol{\omega}_e \times \bar{\boldsymbol{\omega}}_B$ and $\bar{\boldsymbol{\tau}}_B = J\boldsymbol{o}_e^*J^{-1}\bar{\boldsymbol{\tau}}\boldsymbol{o}_e$.

1) Step 1: In the first step, we want $\boldsymbol{\omega}_e$ to track a virtual control law $\boldsymbol{\varphi}_e$ such that $\boldsymbol{o}_e \to 1$ if $\boldsymbol{\omega}_e = \boldsymbol{\varphi}_e$. This virtual control law is chosen as

$$\boldsymbol{\varphi}_e = -k_{\varphi e}\boldsymbol{e}_o, \; k_{\varphi e} > 0, \tag{15}$$

where $\boldsymbol{e}_o \equiv \mathcal{I}\{\boldsymbol{o}_e\} \in \mathbb{H}_\mathrm{p}$. Also, let $e_o \equiv \mathcal{R}\{\boldsymbol{o}_e\} \in \mathcal{R}$.

Lemma 2: Applying the virtual control law (15) in the system (13), the point $\boldsymbol{e}_o = 1$ becomes an asymptotic stable equilibrium point.

Proof: Since $\boldsymbol{o}_e = e_o + \boldsymbol{e}_o$, (13) can be rewritten as

$$\dot{e}_o = -\frac{1}{2}\boldsymbol{e}_\mathrm{o}^\top\boldsymbol{\omega}_e, \quad \dot{\boldsymbol{e}}_o = \frac{1}{2}\left(e_o\boldsymbol{\omega}_e + \boldsymbol{e}_o \times \boldsymbol{\omega}_e\right). \tag{16}$$

Let V_{eo} be a candidate Lyapunov function

$$V_{eo}(\boldsymbol{o}_e) = (1 - e_o)^2 + \boldsymbol{e}_o^\top\boldsymbol{e}_o. \tag{17}$$

The time derivative of (17) is

$$\begin{aligned}\dot{V}_{eo} &= 2\boldsymbol{e}_\mathrm{o}^\top\left[\frac{1}{2}\left(e_o\boldsymbol{\omega}_e + \boldsymbol{e}_o \times \boldsymbol{\omega}_e\right)\right] - 2(1 - e_o)\left[-\frac{1}{2}\boldsymbol{e}_\mathrm{o}^\top\boldsymbol{\omega}_e\right],\\ \dot{V}_{eo} &= \boldsymbol{e}_o^\top\boldsymbol{\omega}_e.\end{aligned} \tag{18}$$

Applying (15) into (13), the time derivative of (17) yields

$$\dot{V}_{eo} = -\,k_{\varphi e}\|\boldsymbol{e}_o\|^2, \tag{19}$$

$$\dot{V}_{eo}(1) = 0, \tag{20}$$

$$\dot{V}_{eo}(\boldsymbol{o}_e) < 0, \; \forall \boldsymbol{o}_e \in \mathbb{H}, \|\boldsymbol{o}_e\| = 1, \boldsymbol{o}_e \neq 1, \tag{21}$$

which guarantees asymptotic convergence of the error $\boldsymbol{o}_e$ to 1, and therefore, ensures $\boldsymbol{o} \to \bar{\boldsymbol{o}}$. ■

2) Step 2: For the last step, let $\boldsymbol{e}_\omega = \boldsymbol{\omega}_e - \boldsymbol{\varphi}_e \in \mathbb{H}_\mathrm{p}$ be the angular velocity error that encompasses this virtual control law. The error system is represented by

$$\dot{\boldsymbol{o}}_e = \frac{1}{2}\boldsymbol{o}_e\boldsymbol{\varphi}_e + \frac{1}{2}\boldsymbol{o}_e\boldsymbol{e}_\omega, \tag{22}$$

$$\dot{\boldsymbol{e}}_\omega = \boldsymbol{\Omega}_e + J^{-1}\boldsymbol{\tau}_e + J^{-1}\boldsymbol{\tau}_d - \dot{\boldsymbol{\varphi}}_e, \tag{23}$$

where $\boldsymbol{\tau}_e \equiv \boldsymbol{\tau} - \bar{\boldsymbol{\tau}}_B$ is its control input.

Following the approach in [18], in order to design the robust adaptive control law, consider

$$\chi_o = \boldsymbol{\tau}_d + J\boldsymbol{\Omega}_e - J\dot{\boldsymbol{\varphi}}_e \tag{24}$$

as a lumped term that contains the bounded disturbance $\boldsymbol{\tau}_d$. Using an indirect method [25], [26], the controller tackles χ_o by focusing only on its bound. Accordingly, the following assumption is considered.

Assumption 1 (Norm bounded disturbances): There exist unknown constants ζ_1 and ζ_2 such that

$$\|\chi_o\| \leq \zeta_1 + \zeta_2\|\boldsymbol{e}_\omega\|, \tag{25}$$

and those constants $\zeta \equiv \begin{bmatrix}\zeta_1 & \zeta_2\end{bmatrix}^T$ belong to a convex set Ξ described by

$$\zeta \in \Xi, \quad \Xi = \{\xi \in \mathbb{R}^2 \mid \alpha(\xi) \leq 0\}, \tag{26}$$

where $\alpha : \mathbb{R}^2 \to \mathbb{R}$ is a smooth function.

These constants are estimated in the controller by adaptive parameters $\hat{\zeta} \equiv \begin{bmatrix}\hat{\zeta}_1 & \hat{\zeta}_2\end{bmatrix}^T$, where $\hat{\zeta}(0) \in \Xi$.

Then, the robust adaptive control law for the error system is given by[1]

$$\boldsymbol{\tau}_e = -k_{eo}\boldsymbol{e}_o - k_{e\omega}\boldsymbol{e}_\omega - \hat{\zeta}_1\mathbf{tanh}(\hat{\zeta}_1\boldsymbol{e}_\omega/\epsilon_o) - \hat{\zeta}_2\boldsymbol{e}_\omega, \quad (27)$$

where $k_{eo}, k_{e\omega}, \epsilon_o > 0$ are scalar gains, and the adaptive parameters $\hat{\zeta}_1, \hat{\zeta}_2 > 0$ have the following update laws:

$$\dot{\hat{\zeta}} = \begin{cases} P\epsilon & \text{if } \alpha(\hat{\zeta}) < 0 \text{ or } \nabla\alpha^T P\epsilon \leq 0, \\ P\epsilon - P\frac{\nabla\alpha\nabla\alpha^T}{\nabla\alpha^T P\nabla\alpha}P\epsilon & \text{otherwise} \end{cases}$$

$$P = \begin{bmatrix}\rho_1 & 0 \\ 0 & \rho_2\end{bmatrix} > 0, \quad \epsilon = \begin{bmatrix}\|\boldsymbol{e}_\omega\| \\ \|\boldsymbol{e}_\omega\|^2\end{bmatrix}, \quad (28)$$

where a projection modification was applied [19].

Lemma 3: Considering Assumption 1, let $V_{eo\omega}$ be the following control Lyapunov function:

$$V_{eo\omega} = k_{eo}V_{eo} + \frac{1}{2}\boldsymbol{e}_\omega^\top J\boldsymbol{e}_\omega + \frac{\tilde{\zeta}_1^2}{2\rho_1} + \frac{\tilde{\zeta}_2^2}{2\rho_2}, \quad (29)$$

where $\tilde{\zeta} \equiv \begin{bmatrix}\tilde{\zeta}_1 & \tilde{\zeta}_2\end{bmatrix}^T = \zeta - \hat{\zeta}$ are estimation errors. By applying (27) in the system (22)-(23), $\dot{V}_{eo\omega} < 0$ if the system is outside the attractive set Δ_o given by

$$\Delta_o = \{(\boldsymbol{e}_o, \boldsymbol{e}_\omega) \mid \|\boldsymbol{e}_o\| \leq \delta_o, \|\boldsymbol{e}_\omega\| \leq \delta_\omega\}, \quad (30)$$

$$\delta_o = \sqrt{\frac{3\kappa\epsilon_o}{k_{eo}k_{\varphi e}}},\ \delta_\omega = \sqrt{\frac{3\kappa\epsilon_o}{k_{e\omega}}}, \quad (31)$$

with $\kappa \approx 0.2785$.

Proof: Consider Lemma 2 and the function (29). The time derivative of $V_{eo\omega}$ is given by

$$\dot{V}_{eo\omega} = -k_{eo}k_{\varphi e}\|\boldsymbol{e}_o\|^2 + k_{eo}\boldsymbol{e}_o^\top\boldsymbol{e}_\omega - \tilde{\zeta}_1\dot{\hat{\zeta}}_1/\rho_1 - \tilde{\zeta}_2\dot{\hat{\zeta}}_2/\rho_2 + \boldsymbol{e}_\omega^\top(J\boldsymbol{\Omega}_e + \boldsymbol{\tau}_d - J\dot{\boldsymbol{\varphi}}_e + \boldsymbol{\tau}_e). \quad (32)$$

For the sake of simplicity, consider for now that the first conditions for $\dot{\hat{\zeta}}$ law in (28) are always met. Later we show that the projection modification [19] does not impact on the result. Then, substituting (27) and (28) in (32) yields

$$\begin{aligned}\dot{V}_{eo\omega} = &- k_{eo}k_{\varphi e}\|\boldsymbol{e}_o\|^2 - k_{e\omega}\|\boldsymbol{e}_\omega\|^2 + \boldsymbol{e}_\omega^\top\chi_o \\ &- \boldsymbol{e}_\omega^\top\hat{\zeta}_1\mathbf{tanh}(\hat{\zeta}_1\boldsymbol{e}_\omega/\epsilon_o) - \hat{\zeta}_2\|\boldsymbol{e}_\omega\|^2 \\ &- \tilde{\zeta}_1\|\boldsymbol{e}_\omega\| - \tilde{\zeta}_2\|\boldsymbol{e}_\omega\|^2. \end{aligned} \quad (33)$$

Considering Assumption 1 leads to

$$\begin{aligned}\dot{V}_{eo\omega} \leq &- k_{eo}k_{\varphi e}\|\boldsymbol{e}_o\|^2 - k_{e\omega}\|\boldsymbol{e}_\omega\|^2 \\ &- \hat{\zeta}_1\|\boldsymbol{e}_\omega\|\mathbf{tanh}(\hat{\zeta}_1\|\boldsymbol{e}\|_\omega/\epsilon_o) + \hat{\zeta}_1\|\boldsymbol{e}_\omega\|. \end{aligned} \quad (34)$$

Using both the following properties, [18], [27], (i) $\|\boldsymbol{q}\| \leq \sum_{i=1}^n |q_i|, \forall\boldsymbol{q} \in \mathbb{R}^n$; and (ii) $0 \leq |a| - a\tanh(a/\varepsilon_p) \leq \kappa\varepsilon_p, \forall a \in \mathbb{R}$; yields:

$$\dot{V}_{eo\omega} \leq -k_{eo}k_{\varphi e}\|\boldsymbol{e}_o\|^2 - k_{e\omega}\|\boldsymbol{e}_\omega\|^2 + 3\kappa\epsilon_o. \quad (35)$$

In which $\dot{V}_{eo\omega} < 0$ for $\|\boldsymbol{e}_o\| > \sqrt{\frac{3\kappa\epsilon_o}{k_{eo}k_{\varphi e}}}$ or $\|\boldsymbol{e}_\omega\| > \sqrt{\frac{3\kappa\epsilon_o}{k_{e\omega}}}$.

When the projection modification is active, *i.e.* the second condition for the update law, $\dot{\hat{\zeta}}$, in (28) is met, there is an extra term in the Lyapunov function derivative $\dot{V}_{eo\omega}$ given by

$$\tilde{\zeta}^T\frac{\nabla\alpha\nabla\alpha^T}{\nabla\alpha^T P\nabla\alpha}P\epsilon. \quad (36)$$

By definition, $\nabla\alpha^T P\epsilon > 0$ when this modification is active and $\tilde{\zeta}^T\nabla\alpha \leq 0$ since Ξ is convex [19]. Therefore, the extra term (36) does not make (35) more positive and ensures that the adaptive gains remain in Ξ [19]. ■

Lemma 4: Considering Assumption 1 and applying (27) in the system (22)-(23), the error system state $(\boldsymbol{e}_o, \boldsymbol{e}_\omega, \tilde{\zeta})$ is uniformly ultimately bounded by

$$\|\boldsymbol{e}_o\|^2 + \|\boldsymbol{e}_\omega\|^2 + \|\tilde{\zeta}\|^2 \leq \frac{k_1 + k_2 + r}{c}, \quad (37)$$

with

$$\begin{aligned} k_1 &= \frac{6\kappa\epsilon_o}{k_{\varphi e}} > 0, \quad k_2 = \frac{3\kappa\epsilon_o\|J\|}{2k_{e\omega}} > 0, \\ r &= \frac{1}{2}\|P^{-1}\|d^2 > 0, \\ c &= \min\{k_{eo}, 0.5\lambda_{\min}(J), 0.5\lambda_{\max}^{-1}(P)\}, \end{aligned}$$

where d is the maximum diameter of Ξ.

Proof: First, notice that the unit norm constraint on the quaternion error $\boldsymbol{o}_e = e_o + \boldsymbol{e}_o$ implies that $|e_o(t)|^2 + \|\boldsymbol{e}_o(t)\|^2 = 1$, $\forall t \in \mathbb{R}$, such that the candidate Lyapunov function (17) can be rewritten as

$$\begin{aligned} V_{eo} &= (1 - e_o)^2 + \|\boldsymbol{e}_o\|^2, \\ &= 2(1 - e_o) = 2\left(1 - \sqrt{1 - \|\boldsymbol{e}_o\|^2}\right), \end{aligned}$$

and

$$\|\boldsymbol{e}_o\| \leq 1 \Rightarrow \|\boldsymbol{e}_o\|^2 \leq V_{eo} \leq 2\|\boldsymbol{e}_o\|^2.$$

These last inequalities are true because $\|\boldsymbol{e}_o\| \leq 1 \Rightarrow (1 - \|\boldsymbol{e}_o\|^2) \leq \sqrt{1 - \|\boldsymbol{e}_o\|^2} \leq 1 - 0.5\|\boldsymbol{e}_o\|^2$. This shows that the candidate Lyapunov function (29) can be rewritten as

$$V_{eo\omega} = a_1 + a_2 + F,$$

where $a_1 = 2k_{eo}\left(1 - \sqrt{1 - \|\boldsymbol{e}_o\|^2}\right) \geq 0$, $a_2 = \frac{1}{2}\boldsymbol{e}_\omega^\top J\boldsymbol{e}_\omega \geq 0$, and $F = \frac{1}{2}\tilde{\zeta}^\top P^{-1}\tilde{\zeta} \geq 0$. From Lemma 3, and the fact that $a_1 \leq 2k_{eo}\|\boldsymbol{e}_o\|^2$, $a_1 > k_1 \Rightarrow \dot{V}_{eo\omega} < 0$, or $a_2 > k_2 \Rightarrow \dot{V}_{eo\omega} < 0$. Thus, $a_1 + a_2 > k_1 + k_2 \Rightarrow \dot{V}_{eo\omega} < 0$, as $a_1 > k_1$ or $a_2 > k_2$.

This means that the set $\Delta = \{(\boldsymbol{e}_o, \boldsymbol{e}_\omega, \tilde{\zeta}) \mid V_{eo\omega} \leq k_1 + k_2 + r\}$ is attractive: if $V_{eo\omega} = a_1 + a_2 + F > k_1 + k_2 + r \Leftrightarrow a_1 + a_2 > k_1 + k_2 + (r - F) > k_1 + k_2 \Rightarrow \dot{V}_{eo\omega} < 0$. It is also positively invariant because, when $V_{eo\omega} = k_1 + k_2 + r$, we also find that $\dot{V}_{eo\omega} < 0$ since $a_1 + a_2 + F = k_1 + k_2 + r \Rightarrow a_1 + a_2 > k_1 + k_2$.

Finally, notice that $V_{eo\omega} \geq c\left(\|\boldsymbol{e}_o\|^2 + \|\boldsymbol{e}_\omega\|^2 + \|\tilde{\zeta}\|^2\right)$, and when the error system state reaches the attractive and positively invariant set Δ defined above, which happens in finite time, condition (37) will be satisfied. ■

[1] The function $\tanh(\boldsymbol{q})$ is defined in terms of exponential maps. It is noteworthy that the bold $\mathbf{tanh}(\boldsymbol{q})$ is an abuse of notation, in which we actually mean the element-wise hyperbolic-tangent, applied to each imaginary field of $\boldsymbol{q}$.

C. Practical system control

The last part of our method is to combine the controller design. Now, we can present the complete controller scheme, which is given by

$$\boldsymbol{\tau} = \bar{\boldsymbol{\tau}}_B + \boldsymbol{\tau}_e, \tag{38}$$

The proposed method yields the following result.

Theorem 1 (Attitude Controller): Considering Assumption 1 and applying (38) in the practical system (1)-(2), the system trajectories asymptotically converge to a control invariant set around the time-varying reference orientation $\boldsymbol{o}_d(t)$.

Proof: Lemmas 1 states that the nominal system (4)-(5) asymptotically converges to the reference orientation. Furthermore, the error between the practical system and the nominal trajectory is constrained as a result of Lemmas 3 and 4. ■

Figure 1 illustrates the idea behind the proposed controller. The target attitude $\boldsymbol{o}_d$ is shown in the middle of the image plotted in continuous lines. Then, the nominal system attitude $\bar{\boldsymbol{o}}$ is plotted in dashed lines. A control law $\bar{\boldsymbol{\tau}}$ aims to asymptotically drive $\bar{\boldsymbol{o}}$ to $\boldsymbol{o}_d$, as shown with the brown arrow. Finally, the practical system attitude $\boldsymbol{o}$ is plotted in dashed-dotted, where a control law $\boldsymbol{\tau}_e$ aims to stabilize $\boldsymbol{o}$ in a region around $\bar{\boldsymbol{o}}$. Combining both control law efforts we obtain equation (38), where Theorem 1 holds.

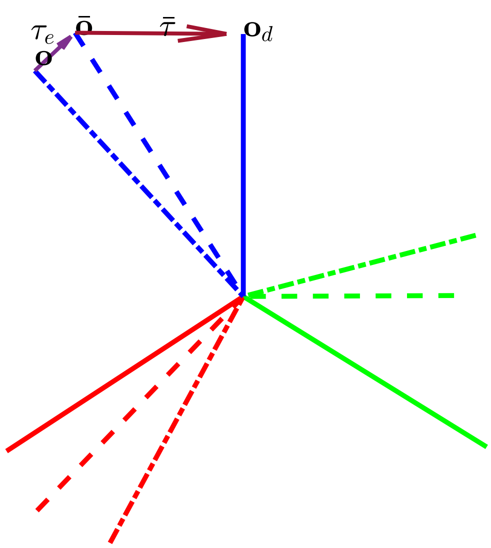

Fig. 1. Illustration of the proposed control method. The reference frame for the target $\boldsymbol{o}_d$ is plotted in continuous lines, the one for the nominal system $\bar{\boldsymbol{o}}$ is plotted in dashed lines and the one for the practical system $\boldsymbol{o}$ is plotted in dashed-dotted lines.

IV. RESULTS

A video with animations, recordings, and more details about the results is available at youtu.be/r-MWOgKWWqo. The code used in this section is available at github.com/ArthurHDN/cdc2024.

A. Simulations

For the simulations, the rigid-body attitude (1)-(2) was controlled to track a reference orientation trajectory given by

$$\begin{aligned}
\boldsymbol{o}_d(t) &= \boldsymbol{o}_1(t)\boldsymbol{o}_2(t),\\
\boldsymbol{o}_1(t) &= \cos\left(\frac{t}{10}\right) + \hat{\boldsymbol{k}}\sin\left(\frac{t}{10}\right),\\
\boldsymbol{o}_2(t) &= \cos\left(\frac{\pi}{6}\right) + \left(\hat{\boldsymbol{\imath}}\cos\left(\frac{t}{5}\right) + \hat{\boldsymbol{\jmath}}\sin\left(\frac{t}{5}\right)\right)\sin\left(\frac{\pi}{6}\right).
\end{aligned}$$

The system's initial conditions were

$$\begin{aligned}
\boldsymbol{o}(0) = \bar{\boldsymbol{o}}(0) &= \cos\left(\frac{1}{2}\cdot\frac{\pi}{3}\right) + \hat{\jmath}\sin\left(\frac{1}{2}\cdot\frac{\pi}{3}\right),\\
\boldsymbol{\omega}(0) = \bar{\boldsymbol{\omega}}(0) &= 0\ \mathrm{rad\,s^{-1}}.
\end{aligned}$$

As for the inertia tensor, we introduced a $+20\%$ parameter estimation error in the controller, given by

$$\begin{aligned}
J &= \begin{bmatrix} 2.3951 & 0 & 0\\ 0 & 2.3951 & 0\\ 0 & 0 & 3.2347 \end{bmatrix}\cdot 10^{-5}\ \mathrm{kg\,m^2},\\
\bar{J} &= 1.2J,
\end{aligned}$$

where J is the actual system inertia and $\bar{J}$ is the inertia used in the controller.

The nominal controller gains were tuned as

$$\begin{aligned}
k_o &= 5\ \mathrm{s^{-2}},\\
K_\omega &= \begin{bmatrix} 10.3813 & -0.0024 & -0.0098\\ -0.0024 & 10.5941 & -0.0003\\ -0.0098 & -0.0003 & 10.5928 \end{bmatrix}\ \mathrm{s^{-1}},
\end{aligned}$$

while the robust controller gains were

$$\begin{aligned}
k_{\phi e} &= 2.5\ \mathrm{s^{-1}},\\
k_{eo} &= 10^{-2}\ \mathrm{N\,m\,rad^{-1}},\\
k_{e\omega} &= 6\cdot 10^{-3}\ \mathrm{N\,m\,s\,rad^{-1}},\\
\epsilon_o &= 2\cdot 10^{-3}\ \ \mathrm{s\,N^{-1}\,m^{-1}\,rad^{-1}},\\
\rho_1 &= 5\cdot 10^{-4}\mathrm{N\,m\,rad^{-1}},\\
\rho_2 &= 10^{-3}\mathrm{N\,m\,s^2\,rad^{-3}}.
\end{aligned}$$

The added disturbances were given by

$$\begin{aligned}
\boldsymbol{\tau}_d &= \left(\hat{\boldsymbol{\imath}}d_x + \hat{\boldsymbol{\jmath}}d_y + \hat{\boldsymbol{k}}d_z\right)\ \mathrm{N\,m},\\
d_x &= \mathcal{N}(0, 5\cdot 10^{-5}),\\
d_y &= \mathcal{N}(0, 5\cdot 10^{-5})\mathbb{1}_{15} + 2.5\cdot 10^{-3}\sin(t/2)\mathbb{1}_{40},\\
d_z &= \mathcal{N}(0, 5\cdot 10^{-5})\mathbb{1}_{65} + 1\cdot 10^{-3}\mathbb{1}_{65},
\end{aligned}$$

where $\mathcal{N}(\mu,\sigma)$ is a Gaussian distribution with mean μ and deviation σ, and $\mathbb{1}_{t_0}$ is the unit time step starting at $t = t_0$. The set Ξ was chosen as a circle according to $\alpha(\xi) = \xi^T\xi - r^2$, with $r = 0.005$.

Fig. 2 shows the attitude, represented in Euler angles for better visualization, in continuous lines with the reference attitude in dashed lines. The system attitude converged to the desired trajectory, keeping a small error below δ_o, as expected.

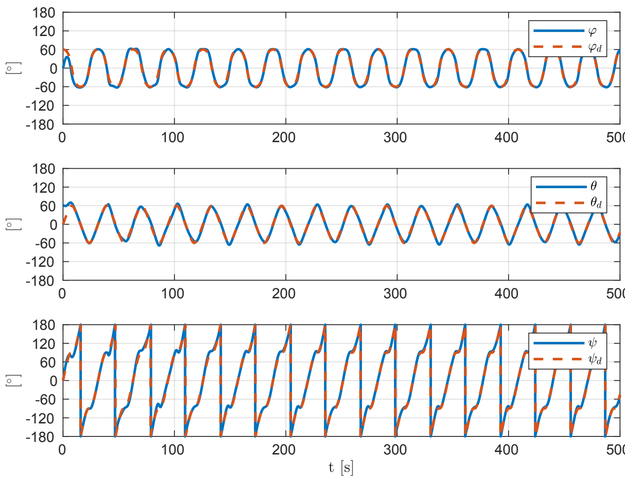

Fig. 2. Simulation: attitude in continuous lines with the reference attitude in dashed lines. For a more readable result, the attitudes were converted to Euler angles: φ, θ, and ψ which corresponds to roll, pitch, and yaw.

The error between the practical and nominal systems stayed in the set Δ_o, as shown in Fig. 3.

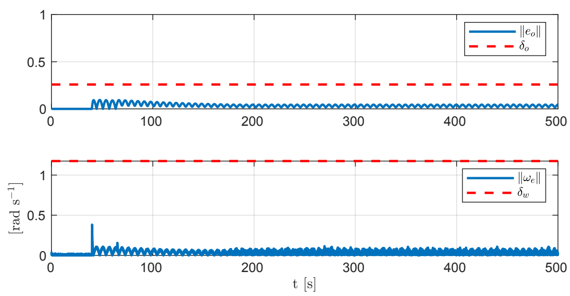

Fig. 3. Simulation: norm of attitude error between practical and nominal systems (top), and norm of angular velocity error between practical and nominal systems (bottom).

As for the norm of the error between the practical system and the reference attitudes, denoted by $\|\mathcal{I}\{\boldsymbol{o}_d^*\boldsymbol{o}\}\|$, is shown by Fig. 4.

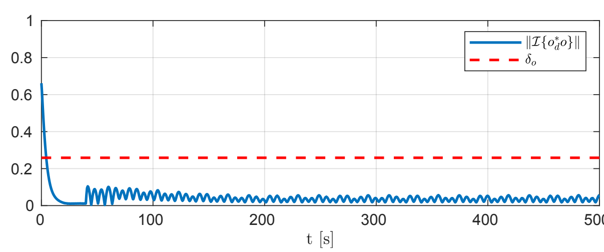

Fig. 4. Simulation: norm of attitude error between the practical system and the reference.

Fig. 5 shows the evolution in time of the adaptive gains, which stayed in Ξ, and therefore, not drifting to infinity.

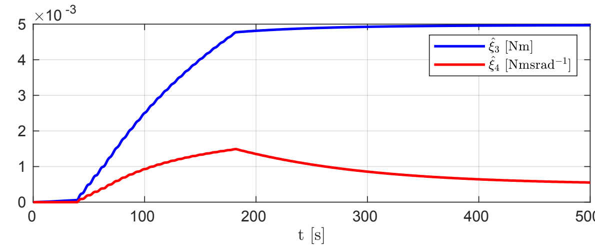

Fig. 5. Simulation: evolution in time of adaptive gains.

To highlight the superiority of the combined nominal and robust adaptive controller, we repeated the same simulation scenario but employed only the nominal controller to the system, which achieved a worse and unstable performance. This can be seen by comparing Fig. 2 with Fig. 6 below.

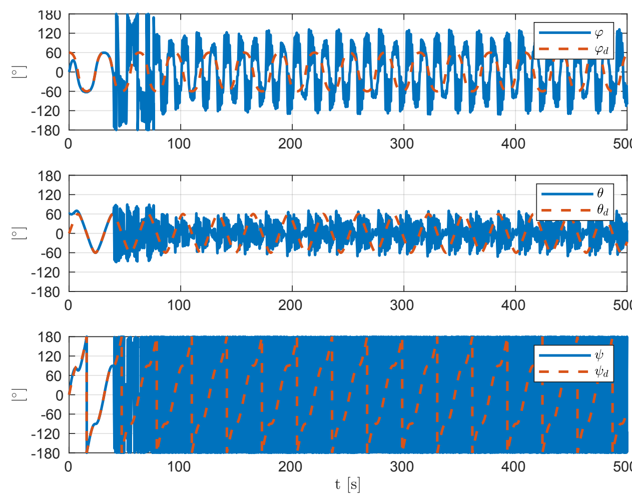

Fig. 6. Simulation: attitude when employing only the nominal controller. in continuous lines with the reference attitude in dashed lines. For a more readable result, the attitudes were converted to Euler angles: φ, θ, and ψ which corresponds to roll, pitch, and yaw.

B. Experiments

For the experiments, a Crazyflie platform[2] was attached to a gimbal ring test-bench to allow the quadcopter to change its orientation without colliding or changing its position. We repeated the experiment with three different attitude references passed to the controller, which achieved good results. Besides the inherited uncertainties of the experiment, the system sometimes was strongly externally disturbed by shaking and hitting the test-bench as can be observed in the afore mentioned video.

Fig. 7 shows the attitude in continuous lines and the attitude reference in dashed lines.

[2]Crazyflie 2.1 available at bitcraze.io.

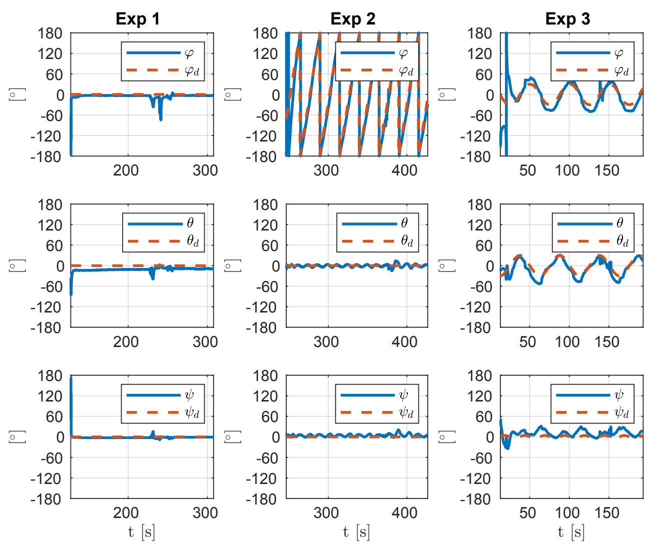

Fig. 7. Experiments: attitude states in continuous lines and the attitude references in dashed lines.

V. CONCLUSION

In this work, we proposed a rigid-body attitude control scheme for tracking time-varying orientation references under the presence of magnitude-bounded disturbances. Our method consists in combining a nominal controller with a robust adaptive backstepping control law to ensure the system converges to a limited region around the reference attitude.

In addition, the adaptive gains do not drift to infinity, and the nominal asymptotic convergence is ensured to the time-varying reference, while also guaranteeing an ultimate bounded tracking error in the disturbed cases with formal proofs. Simulations and experiments with a quadcopter validate our control strategy.

This method, requires a design of a region for the adaptive gains to reside within given the projection modification [19]. If this region is poorly designed and becomes smaller than required, it may not contain values to properly mitigate the disturbances. If the region is big, the gains might increase and the behaviour of the system may approach a high-gain control method.

For future work, we propose to extend this controller by considering also the translation dynamics of the quadcopter.

REFERENCES

[1] D. Invernizzi, "Modeling and attitude control of spacecraft with an unbalanced rotating device," *IEEE Control Systems Letters*, vol. 7, pp. 466–471, 2023.

[2] J. Giordano and A. Cenedese, "Quaternion-based non-singular terminal sliding mode control for a satellite-mounted space manipulator," *IEEE Control Systems Letters*, vol. 7, pp. 2659–2664, 2023.

[3] K. Patnaik and W. Zhang, "Adaptive attitude control for foldable quadrotors," *IEEE Control Systems Letters*, vol. 7, pp. 1291–1296, 2023.

[4] F. Ahmed, L. Sobiesiak, and J. R. Forbes, "Cascaded model predictive control of a tandem-rotor helicopter," *IEEE Control Systems Letters*, vol. 7, pp. 1345–1350, 2023.

[5] S. Iwata, S. Sahashi, and T. Hasegawa, "Verification of visual attitude control for outdoor autonomous mobile robots," in *2013 10th International Conference on Ubiquitous Robots and Ambient Intelligence (URAI)*, pp. 319–320, 2013.

[6] S. Bouabdallah, A. Noth, and R. Siegwart, "PID vs LQ control techniques applied to an indoor micro quadrotor," in *2004 IEEE/RSJ International Conference on Intelligent Robots and Systems (IROS) (IEEE Cat. No.04CH37566)*, vol. 3, pp. 2451–2456 vol.3, 2004.

[7] N. Bao, X. Ran, Z. Wu, Y. Xue, and K. Wang, "Research on attitude controller of quadcopter based on cascade PID control algorithm," in *2017 IEEE 2nd Information Technology, Networking, Electronic and Automation Control Conference (ITNEC)*, pp. 1493–1497, 2017.

[8] D. Mayne, M. Seron, and S. Raković, "Robust model predictive control of constrained linear systems with bounded disturbances," *Automatica*, vol. 41, pp. 219–224, Feb. 2005.

[9] B. Yang, F. He, and Y. Yao, "MPC-based design of on-off control law of the attitude control thruster," in *2008 27th Chinese Control Conference*, pp. 539–543, 2008.

[10] L. Sun and W. Huo, "Robust adaptive attitude tracking for satellites with constrained control inputs," in *Proceedings of the 32nd Chinese Control Conference*, pp. 2885–2890, 2013.

[11] A. H. D. Nunes, G. V. Raffo, and L. C. A. Pimenta, "Integrated vector field and backstepping control for quadcopters," in *2023 IEEE International Conference on Robotics and Automation (ICRA)*, pp. 1256–1262, 2023.

[12] G. F. Salierno, "Whole-body backstepping control of a quadrotor UAV for trajectory tracking," Master's thesis, Universidade Federal de Minas Gerais, 2018.

[13] G. F. Salierno and G. V. Raffo, "Whole-body backstepping control with integral action of a quadrotor UAV," in *Proceedings of the XIII Brazilian Symposium on Intelligent Automation (SBAI 2017), Porto Alegre, Brazil*, pp. 2157–2164, 2017.

[14] S. Bouabdallah and R. Siegwart, "Backstepping and sliding-mode techniques applied to an indoor micro quadrotor," in *Proceedings of the 2005 IEEE International Conference on Robotics and Automation*, pp. 2247–2252, 2005.

[15] M. Huang, B. Xian, C. Diao, K. Yang, and Y. Feng, "Adaptive tracking control of underactuated quadrotor unmanned aerial vehicles via backstepping," in *Proceedings of the 2010 American Control Conference*, pp. 2076–2081, 2010.

[16] I. A. Raptis, K. P. Valavanis, and W. A. Moreno, "A novel nonlinear backstepping controller design for helicopters using the rotation matrix," *IEEE Transactions on Control Systems Technology*, vol. 19, no. 2, pp. 465–473, 2011.

[17] C. K. Tan, J. Wang, Y. C. Paw, and T. Y. Ng, "Tracking of a moving ground target by a quadrotor using a backstepping approach based on a full state cascaded dynamics," *Applied Soft Computing*, vol. 47, pp. 47–62, 2016.

[18] L. Zhang, H. Wang, Y. Zhu, and J. Yang, "Tube-based attitude control of rigid-bodies with magnitude-bounded disturbances," *Automatica*, vol. 133, p. 109845, Nov. 2021.

[19] J. A. Farrell and M. M. Polycarpou, *Adaptive approximation based control: unifying neural, fuzzy and traditional adaptive approximation approaches*. John Wiley & Sons, 2006.

[20] F. F. Afonso Silva, J. José Quiroz-Omaña, and B. Vilhena Adorno, "Dynamics of mobile manipulators using dual quaternion algebra," *Journal of Mechanisms and Robotics*, vol. 14, no. 6, p. 061005, 2022.

[21] Y.-B. Jia, "Quaternions," *Com S*, vol. 477, p. 577, 2019.

[22] B. Vilhena Adorno, "Robot Kinematic Modeling and Control Based on Dual Quaternion Algebra — Part I: Fundamentals.." working paper or preprint, Feb. 2017.

[23] J. B. Kuipers, *Quaternions and rotation sequences: a primer with applications to orbits, aerospace, and virtual reality*. Princeton university press, 1999.

[24] H. K. Khalil, *Nonlinear Systems*. Prentice Hall, third ed., 2002.

[25] Z. Zhu, Y. Xia, and M. Fu, "Adaptive sliding mode control for attitude stabilization with actuator saturation," *IEEE Transactions on Industrial Electronics*, vol. 58, no. 10, pp. 4898–4907, 2011.

[26] W. Cai, X. H. Liao, and Y. D. Song, "Indirect robust adaptive fault -tolerant control for attitude tracking of spacecraft," *Journal of Guidance, Control, and Dynamics*, vol. 31, pp. 1456–1463, Sept. 2008.

[27] M. Polycarpou and P. Ioannou, "A robust adaptive nonlinear control design," *Automatica*, vol. 32, pp. 423–427, Mar. 1996.